Tr. J. of Physics
23 (1999) , 565 – 575.

Well-width dependence of warm electron relaxation and interface roughness scattering in GaAs/Ga1-xAlxAs multiple quantum wells

M. CANKURTARAN, H. ÇELİK, E. TIRAŞ and A. BAYRAKLI
Hacettepe University, Department of Physics,
Beytepe, 06532 Ankara-TURKEY

N. BALKAN
University of Essex, Department of Physics, Colchester, U.K.

Received 01.03.1999

Abstract

We review our recent results concerning the well-width dependence of the acoustic-phonon-assisted energy relaxation of two-dimensional (2D) warm electrons in modulation-doped GaAs/$Ga_{1-x}Al_xAs$ multiple quantum wells. Electron energy-loss rates via the emission of acoustic phonons are determined from the amplitude of Shubnikov-de Haas (SdH) oscillations, measured as a function of lattice temperature and applied electric field. Experimental results are compared with the existing theoretical models that involve deformation-potential and screened and unscreened piezoelectric scattering.

Well-width dependence of the quantum and transport mobilities of 2D electrons in the same samples have also been determined by measuring the quantum oscillations in both the magnetoresistance and Hall resistance. Our results confirm earlier independent conclusions that the momentum relaxation in GaAs/$Ga_{1-x}Al_xAs$ multiple quantum wells is limited mainly by interface roughness scattering. A new theoretical modelling has been proposed and used to estimate the interface roughness parameters from the measured quantum and transport mobilities of 2D electrons.

1. Introduction

Measurements of electron temperatures (T_E) from the Shubnikov-de Haas oscillations as a function of the applied electric field have been commonly used to determine the power loss of warm electrons in both three-dimensional [1] and two-dimensional (2D) systems [2-7].

At low magnetic fields, the SdH oscillations are well described by [8]:

$$\frac{\Delta\rho_{xx}}{\rho_0} = \sum_{r=1}^{\infty} b_r \cos(\frac{2\pi r E_F}{\hbar\omega_c} - r\pi), \tag{1}$$

where $b_r = D(r\chi)\,\exp(-r\pi/\mu_q B)\cos(r\pi\nu)$, $D(r\chi) = r\chi/\sin h(r\chi)$, and $\chi = 2\pi^2 k_B T/\hbar\,\bar{\omega}_c$. Here $\Delta\rho_{xx}$, ρ_0, B, E_F, ω_c, m^*, μ_q, k_B, $\hbar, r, \nu$, and τ_q are the oscillatory magnetoresistivity, zero-magnetic field resistivity, magnetic field, Fermi energy, cyclotron frequency ($\omega_c = eB/m^*$), the electron effective mass in the first subband, quantum mobility, Boltzmann constant, Planck constant, harmonic index, the spin-splitting factor, and the quantum lifetime, respectively. The factor $D(r\chi)$ describes the temperature dependence of oscillation amplitude. The exponential factor, $\exp(-r\pi/\mu_q B)$, describes the decay of the amplitude of oscillations with magnetic field and enables the determination of the value of the quantum lifetime ($\tau_q = m^*\mu_q/e$).

Recent measurements of the power loss as a function of quantum well-width in GaAs/$Ga_{1-x}Al_xAs$ MQW structures addressed a number of uncertainties associated with the cooling mechanisms of warm electrons [7, 9-17]. Here we review some of our recent results concerning the well-width dependence of the acoustic-phonon-assisted energy relaxation of two-dimensional (2D) warm electrons in GaAs/$Ga_{1-x}Al_xAs$ multiple quantum wells with well widths in the range between L= 51 and 145 Å.

We also present the results of our studies concerning the well-width dependence of the quantum (μ_q) and transport (μ_t) mobilities of electrons in GaAs/$Ga_{1-x}Al_xAs$ multiple quantum wells [18, 19]. The results confirm earlier independent conclusions that the momentum relaxation in GaAs/$Ga_{1-x}Al_xAs$ multiple quantum wells is limited mainly by interface roughness scattering.

2. Experimental Procedures

The modulation-doped GaAs/$Ga_{1-x}Al_xAs$ multiple quantum wells were grown by the MBE technique. The $Ga_{1-x}Al_xAs$ barrier layers were doped with Si to a level of 7×10^{23} m^{-3}. The samples were fabricated in the Hall bar geometry and ohmic contacts were formed by diffusing Au/Ge/Ni alloy to all the layers. All the structural and doping parameters were nominally identical except for the quantum well width (L_z) which was varied from 51 to 145 Å (Table 1). All the samples used in the investigations are highly degenerate with 2D electron densities in the range of $\sim 1\times10^6$ m^{-2}.

Magnetoresistance and Hall resistance were measured simultaneously as a function of magnetic field B (0 to 2.3 Tesla) at liquid-helium temperatures (1.5 to 4.2 K) (Figure 1). For a 2D electron gas $\rho_{xx} = R_{xx}b/L$ and $\rho_{xy} = R_{xy}$, where b (=0.375 mm) and L (=1.5 mm) denote the width and length of the Hall bar between the voltage contacts, respectively. The current ($1\mu A < I < 7mA$) flow was in the plane of the MQW and steady and uniform magnetic field was applied perpendicular to the 2D electron gas. The current source and the voltmeter were used to measure the voltages V_{xx} and V_{xy} corresponding to the magnetoresistance (R_{xx}) and the Hall resistance (R_{xy}), respectively. The data were taken at equal intervals of 1/B. Further details of the experimental and data analysis procedures were given in reference 20.

Table 1. Samples parameters of the modulation-doped GaAs/$Ga_{1-x}Al_xAs$ multiple quantum wells.

Sample	x (%)	Number of quantum wells	Undoped GaAs Well width, $L_z(\AA)$	Undoped $Ga_{1-x}Al_xAs$ spacer thickness(Å)	Si-doped $Ga_{1-x}Al_xAs$ barrier thickness(Å)	First subband energy, E_1 (meV)
C579	32	10	51	110	75	73.7
ES2	33	10	75	110	75	45.5
C581	32	10	78	110	75	43.1
568	32	10	106	110	75	27.7
C580	32	10	145	110	75	16.9

Table 2. . In-plane effective mass (m^*), Fermi energy (E_F), electron density (n_{2D}), Hall density (n_H), quantum mobility (μ_q), Hall mobility (μ_H), transport mobility (μ_t) of the 2D electrons for all the samples studied and the lowest lattice temperature (T_o) of measurements.

Sample	L_z (Å)	m^* (m_0)	E_F (meV)	n_{2D} ($10^{16} m^{-2}$)	n_H ($10^{17} m^{-2}$)	μ_q ($m^2 V^{-1} s^{-1}$)	μ_H ($m^2 V^{-1} s^{-1}$)	μ_t ($m^2 V^{-1} s^{-1}$)	T_0 (K)
C579	51	0.0746	31.7	0.98	0.94	0.53	2.43	1.25	1.55
ES2	75	0.0725	38.0	1.08	1.17	0.88	2.98	1.26	1.70
C581	78	0.0717	37.5	1.11	1.07	0.82	3.75	1.08	1.64
C568	106	0.0655	41.2	1.12	1.09	0.56	2.42	0.80	1.70
580	145	0.0657	38.3	1.05	1.18	3.09	2.58	0.99	1.57

3. Experimental Results and Discussion

Figure 2 shows a typical example for the magnetoresistance (R_{xx}) measurements as recorded. It is evident that the oscillatory effect is superimposed on a monotonic component, which causes difficulty in the determination of oscillation amplitude. A widely used method to exclude the effects of the background magnetoresistance and to extract the SdH oscillations is to calculate the negative second derivative of the raw experimental data with respect to the magnetic field ($-\partial^2 R_{xx}/\partial B^2$) [7,18,19]. The negative second derivative of R_{xx} is shown in Figure 2. The Fourier analysis of SdH oscillations confirms that, for each MQW sample studied, only the first subband is populated and that the contribution of higher harmonics is negligible [18]. The fact that the SdH oscillations contains only one period also implies that all the parallel connected quantum wells exhibit almost the same 2D electron density in the populated ground state.

The in-plane electron effective mass (m^*) and the 2D electron density (n_{2D}) required in the calculation of power loss have been obtained from amplitude and period measurements of Shubnikov-de Haas oscillations and are given in Table 2. The Hall coefficient measures the total areal density of carriers (n_H) within a given sample. The values obtained for n_H are also given in Table 2. In all our samples the ratio n_H/n_{2D} is about ten (= the number of quantum wells) within the experimental accuracy. These results indicate that the 2D electron densities are identical in all the quantum wells in each sample and only these electrons contribute to transport properties, thus, parallel conduction is negligible [19].

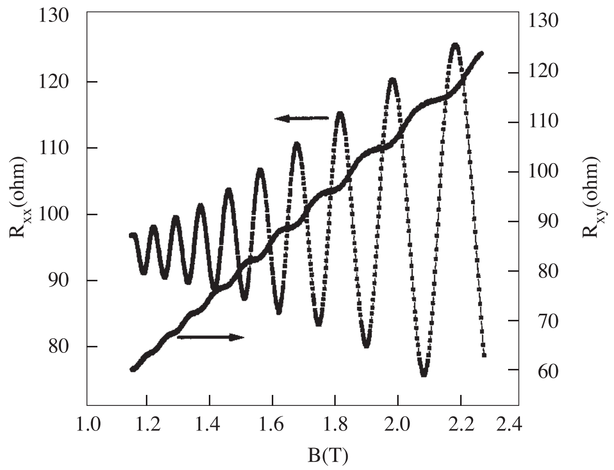

Figure 1. Magnetoresistance (R_{xx}) and Hall resistance (R_{xy}) as a function of magnetic field for sample C580 measured at 4.2 K [19].

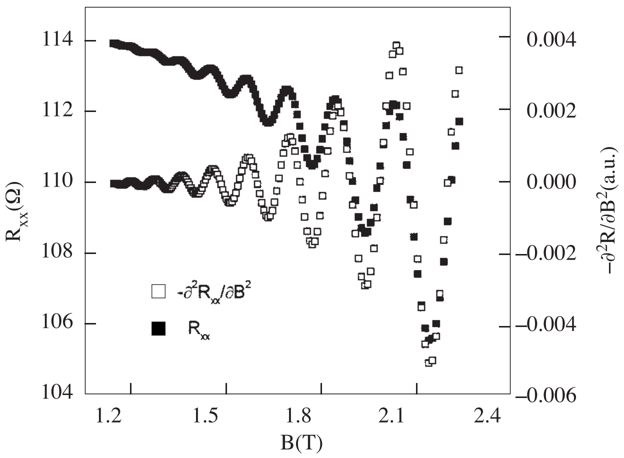

Figure 2. Magnetoresistance and its negative second derivative measured at 4.2 K in sample C579.

Examples for the results of measurements of SdH oscillations as functions of (i) the applied electric field at a fixed lattice temperature T_0 (the lowest of the lattice temperature range in Table 2) and (ii) the lattice temperature T_L in the range $T_0 < T_L < 4.2$ K at a fixed electric field E_0 (that was low enough to ensure ohmic conditions and hence to avoid carrier heating) are shown, respectively, in Figures 3 and 4.

The thermal damping of the oscillations, at a fixed magnetic field is determined by the temperature, magnetic field and the effective electron mass

$$\frac{A(T_L)}{A(T_0)} = \frac{T_L \cdot \sinh(\frac{2\pi^2 k_B m^* T_0}{\hbar e B_n})}{T_0 \cdot \sinh(\frac{2\pi^2 k_B m^* T_L}{\hbar e B_n})} \tag{2}$$

where $A(T_L)$ and $A(T_0)$ are the amplitudes of the oscillation peaks observed at a magnetic field (B_n) at temperatures T_L and T_0.

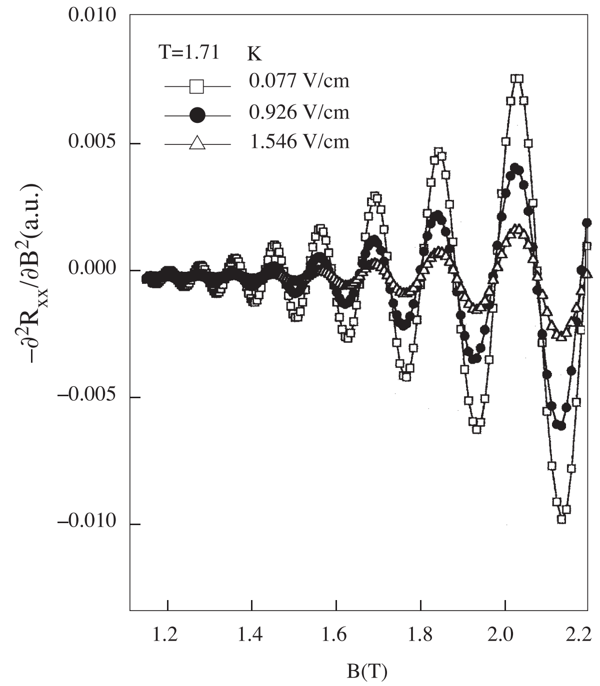

Figure 3. Experimental recordings of the SdH oscillations as a function of the applied electric field in sample C579.

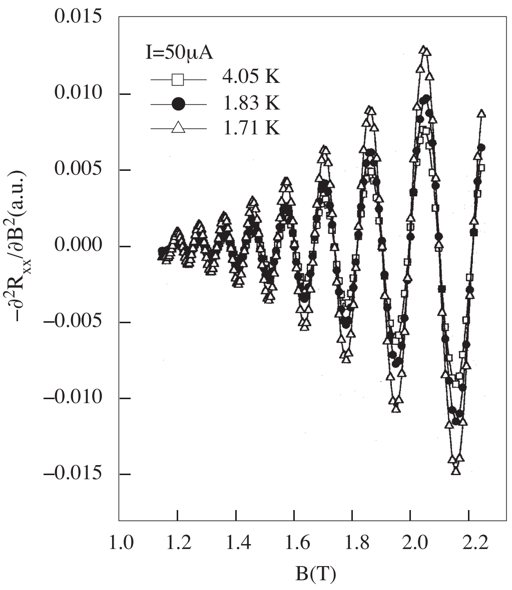

Figure 4. Experimental recordings of the SdH oscillations as a function of lattice temperature in sample C579.

The change in the amplitude of SdH oscillations with electric field can be described in terms of the electric field induced electron heating, then in equation (2), T_L can be replaced by an electron temperature (T_E) and, therefore, the electron temperatures can be determined by comparing, directly, the relative amplitudes of the oscillations plotted as functions of the electric field and lattice temperature [7]:

$$\left[\frac{A(T_L)}{A(T_0)}\right]_{E=E_0} = \left[\frac{A(E)}{A(E_0)}\right]_{T_L=T_0} \tag{3}$$

where E_0 and T_0 are the lowest applied electric field and the lowest lattice temperature of the measurements (Figure 5).

In the steady state, the power loss from the warm electrons to the lattice by the emission of acoustic phonons equals to the power supplied by the applied electric field and can be calculated from the steady state energy balance equation [3],

$$p = e\mu_H(E)^2 \tag{4}$$

where p, μ_H and E are the energy loss/supply rate per electron, electric field dependent electron mobility (which is found to be almost independent of E and T_L in the ranges $E < 1$ V/cm and $1.5\ K < T_L < 4.2K$), and the applied electric field respectively. Power loss versus electron temperature is plotted in Figure 6 for all the samples studied. In order to show the well width dependence clearly, we have plotted in Figure 7 the power loss as a function of the well width at $T_E = 4.2$ K. There is a clear reduction in the power loss with increasing well width up to $L_z = 106\AA$. However, although very limited data is available for wider wells ($L_z \geq 100\AA$) the indication is that the power loss tends to increase as the well width increases and as the electrons acquire more of a quasi 3D characteristic [21].

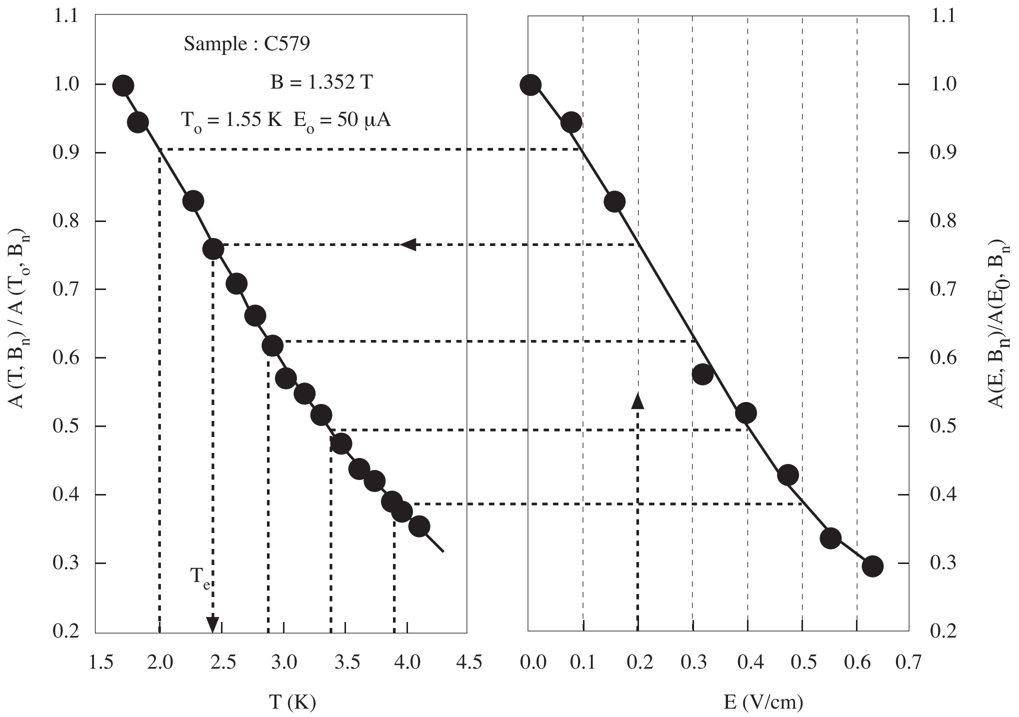

Figure 5. The electron temperature is obtained by comparing the lattice temperature and electric field dependencies of the amplitude of SdH oscillations.

Both the magnitude and the electron temperature dependence of the power loss vary significantly from one sample to another. Since the barrier parameters and 2D carrier densities of all the samples are identical within 10%, the observed variation of the power loss should be associated with the only variable parameter, i.e. the quantum well width, L_z. At all electron temperatures, the power loss tends to increase as the confinement increases for $L_z \leq 100\AA$ (as the electrons acquire more of a 2D character). The 2D analytical expression represents well the electron temperature dependence of power loss [7]. However, they overestimate the magnitude of the power loss, that is, the acoustic phonons are not as efficient in cooling the electrons as predicted theoretically. The 3D calculations describe well the experimental results for wider wells [7].

All models considered fail to predict the magnitude of the power loss, especially for narrow wells. Possible reasons for the discrepancy might be the infinite quantum well approximation used in the theoretical models and that the existing theories use the bulk phonon approximation. However, electron-confined acoustic mode scattering rates for narrow quantum wells may be different from that obtained by using the bulk phonon approximation.

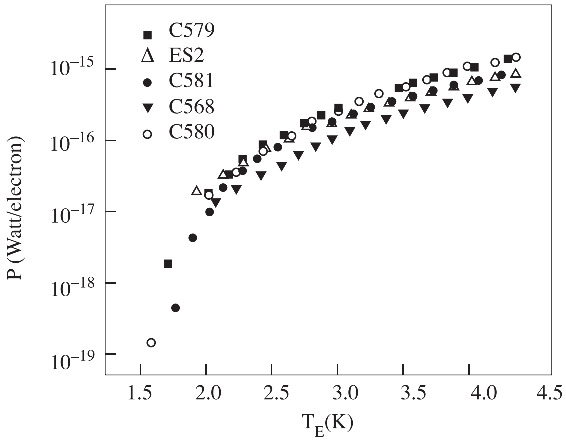

Figure 6. The power loss per electron versus electron temperature for all the samples studied [7].

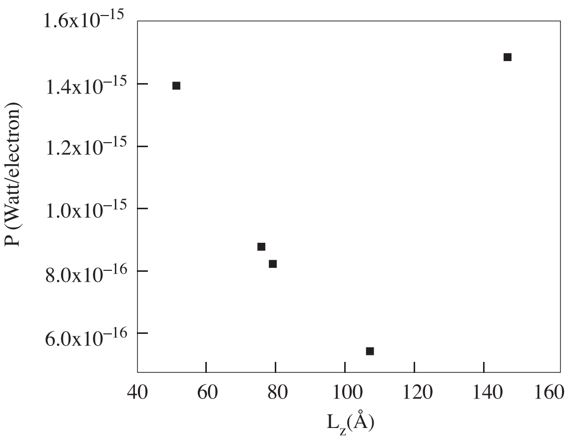

Figure 7. Quantum well - width dependence of power loss per electron at electron temperature 4.2 K.

The relative strengths of the polar and nonpolar components of the 2D loss rates need to considered as well. For all the samples investigated, the nonpolar component of the power loss for the 2D analytical calculations predicts best the experimental temperature dependence and the observed well-width dependence of the power loss [7]. In 2D theoretical models, the piezoelectric scattering rates are somewhat overestimated.

The screening effect has been introduced in the theoretical calculations since screening would reduce the magnitude of the theoretical energy loss rates. It has been shown [21] that both static and dynamic screening give similar results and that the screening does reduce the magnitude of the power loss, with a small effect on the shape of the power loss versus L_z curve. However the inclusion of the static and dynamic screening fails to predict the observed power loss. The population or scattering of electrons into another subband would be possible explanation for the discrepancy. However, n_{2D} and T_L at which the measurements were made are too low for this to occur.

Well-width dependence of the quantum and transport mobilities of 2D electrons in GaAs/Ga$_{1-x}$Al$_x$As MQWs has also been investigated. Experimental results are obtained from the amplitude analysis of oscillations in magnetoresistance and Hall resistance [19]. The values of quantum mobility (μ_q), Hall mobility (μ_H) and transport mobility (μ_t) for all the sample are given in Table 2. The values obtained for μ_q, μ_t and μ_H do not show a systematic dependence on the quantum well width (Figure 8). The values found for μ_t are significantly smaller than those of the Hall mobility (μ_H) obtained in the ohmic regime at low magnetic fields. The discrepancy between μ_t and μ_H has been explained [21] in terms of a transport lifetime τ_t that depends on the electron energy due to the scattering of electrons by interface roughness in the quantum wells.

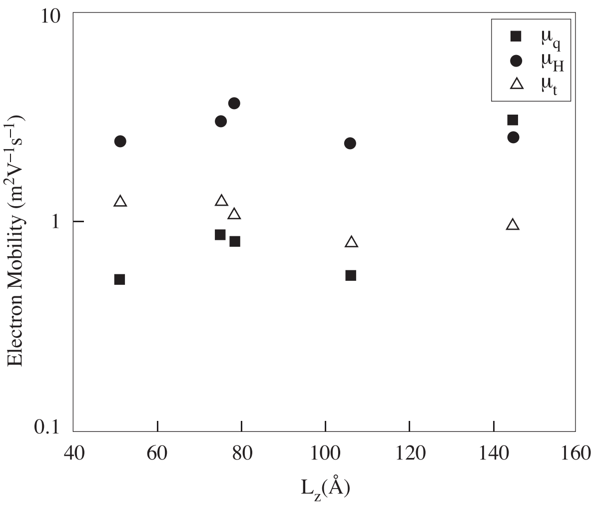

Figure 8. Low temperature electron mobilities versus quantum well width of the samples studied.

We proposed a new theoretical model that estimates the interface roughness parameters from the measured quantum and transport mobilities. The details of the model are discussed elsewhere [22]. The calculations are carried out for a range of layer fluctuations of width (Δ) and lateral size (Λ), as to obtain the best fit to the experimental results for individual samples. These calculations are reported in the current proceedings by Gupta

[23]. Briefly the results indicate that the interface roughness scattering limits equally both quantum and transport mobilities at low temperatures, and that the nature of scattering by interface roughness (small or large angle) depends not only on the size and the width of the fluctuations but also on the spatial distribution of these fluctuations.

Concluding remarks

Well-width dependence of the acoustic-phonon-assisted energy relaxation of 2D warm electrons in GaAs/$Ga_{1-x}Al_xAs$ multiple quantum wells is reported. Experimental results are compared with the existing theoretical models that involve piezoelectric and deformation-potential scattering and also the effects of static and dynamic screening of the piezoelectric interaction. It is shown that screening only slightly modifies the predictions of the approximate calculations. Well-width dependence of quantum and transport mobilities of 2D electrons have been measured and compared by a model previously proposed by us. The model estimates the interface roughness parameters from the measured mobilities. The values found for μ_t are significantly smaller than those of the Hall mobility (μ_H). The discrepancy between μ_t and μ_H has been explained in terms of a transport lifetime τ_t that depends on the electron energy due to the scattering of electrons by interface roughness in the quantum wells.

Acknowledgments

We are grateful to TÜBİTAK (TBAG-1193) and EPSRC for financial support.

References

[1] G. Bauer and H. Kahlert, Phys. Rev. B, 5 (1972) 566.

[2] M. J. Barlow, B. K. Ridley, M. J. Kane and S. J. Bass, Solid State Electron, 31 (1988) 501.

[3] M. E. Daniels, B. K. Ridley, and E. Emeny, Solid State Electron., 32 (1989) 1207.

[4] D. R. Leadley, R. J. Nicholas, J.J. Harris and C. T. Foxon, Semicond. Sci. Technol, 4 (1989) 879.

[5] B. K. Ridley, Rep. Prog. Phys., 54 (1991) 169.

[6] G. Stöger, G. Brunthaler, G. Bauer, K. Ismail, B. S. Meyerson, J. Lutz and F. Kuchar, Semicond. Sci. Technol., 9 (1994) 765.

[7] N. Balkan, H. Çelik, A. J. Vickers, M. Cankurtaran, Phys. Rev. B, 52 (1995) 17210.

[8] T. Ando, A. B. Fowler, F. Stern, Rev. Mod. Phys., 54 (1982) 540.

[9] H. Sakaki, K. Hirakawa, J. Yoshino, S. P. Svenson, Y. Sekiguchi, T. Hotta and S. Nishi, Surface Sci., 142 (1984) 306.

[10] K. Hirakawa, H. Sakaki, App. Phys. Lett., 49 (1986) 889.

[11] K. P. Martin, R. J. Higgins and J. S. L. Rascal, Surface Sci. , 196 (1988) 323.

[12] A. M. Kresschuk, M. Martinov Yu, T. A. Polyanskaya, I. G. Savd'ev, I. I. Saidashev, A. Shik Ya and V. Yu Shmartsev, Solid State Comm., 65 (1988) 1189.

[13] Y. Kodaira, H. Kuwano and K. Tsubaki, App. Phys. Lett., 54 (1988) 2474.

[14] D. R. Leadley, R. J. Nicholas, J. J. Harris and C. T. Foxon, Solid State Elect., 32 (1989) 1473.

[15] R. Fletcher, J.J.Harris, C. T. Foxon, and R. Stoner, Phys.Rev. B,45 (1992) 6659.

[16] A. J. Vickers, Phys. Rev. , B 46 (1992) 13315.

[17] M. Ç. Arıkan, A. Straw and N. Balkan, J. Appl. Phys., 74 (1993) 6261.

[18] H. Çelik, M. Cankurtaran, A. Bayraklı, E. Tıraş and N. Balkan, Semicond. Sci. Technol., 12 (1997) 389.

[19] M. Cankurtaran, H. Çelik, E. Tıraş, A. Bayraklı and N. Balkan, Phys. Stat. Sol. (b), 207 (1998) 139.

[20] H. Çelik, N.Balkan, M. Cankurtaran, A. Bayraklı, Y. Öner, İki Boyutlu Sistemlerde Shubnikov-de Haas Osilasyonları Ölçümleri, TÜBİTAK-TBAG project, No.1193, 1995 (in Turkish)

[21] C. Bennett, N. Balkan, B. Tanatar, H. Celik, M. Cankurtaran, Superlattices and Microstructures, 24 (1998) 25.

[22] N. Balkan, R. Gupta, M. Cankurtaran, H. Çelik, A. Bayraklı, E. Tıraş, M. Ç. Arıkan, Superlattices and Microstructures,22 (1997) 263.

[23] R.Gupta, V. International Research Workshop Low Dimensional Semiconductors: Physics and Devices, 8-11 September 1998, Antalya, Turkey, Abstract Book, p-op3.